JOURNAL OF MATERIALS SCIENCE **38** (2003) 2311 – 2319

An investigation into the amorphous phase separation characteristics of an ionomer glass series and a sodium-boro-silicate glass system

A. RAFFERTY
Department of Materials Science and Technology, University of Limerick, Ireland

R. G. HILL
Department of Materials, Imperial College London, SW7 2BP, UK
E-mail: r.hill@ic.ac.uk

D. WOOD
Division of Restorative Dentistry, Leeds Dental Institute, University of Leeds, Clarendon Way, Leeds LS2 9LU, UK

Amorphous phase separation of ionomer glasses, also known as fluoro-phospho-alumino-silicate glasses, of generic composition SiO_2-Al_2O_3-P_2O_5-CaO-CaF_2 were investigated. A sodium-boro-silicate glass system, which is known to undergo amorphous phase separation was also investigated. High Temperature Dynamic-Mechanical Thermal Analysis (DMTA), combined Differential Thermal Analysis/Thermo Gravimetric Analysis (DTA/TGA) and Scanning Electron Microscopy (SEM) were the principal analytical techniques used in this study. High temperature DMTA was used to measure the glass transition temperatures (T_g) of the original starting glass compositions, as well as being able to follow amorphous phase separation (APS) within the glass. High temperature DMTA traces of both the ionomer glasses and the sodium-boro-silicate glasses exhibited two maxima in tan δ, corresponding to two glass transition temperatures and demonstrating that amorphous phase separation of the parent glass into two glass phases had occurred. DTA/TGA of the ionomer glasses detected a glass transition and two crystallisation peaks for apatite and mullite, accompanied by a gradual weight loss of 1–3% on passing through the crystallisation region. The sodium-boro-silicate base glass showed no evidence of a glass transition, but a prominent glass transition was detected for a second sample which had undergone a heat-treatment of 240 min at 580°C. SEM analysis of the ionomer glass compositions revealed smooth spherical droplets of 2–15 nm while the background morphology appeared rough and speckled. A classic interconnected structure was observed for the sodium-boro-silicate glass.

1. Introduction

Phase transformations in glasses are due to thermodynamic drives for the reduction of free energy. Amorphous phase separation can aid subsequent crystallisation by producing a phase with a greater tendency to nucleate than the initial glass. When phase separation occurs below the liquidus, it is known as metastable immiscibility. There are two routes to the formation of discrete phases by metastable phase separation; either by a nucleation process or by spinodal decomposition. The nucleation and growth mechanism has been characterised by many authors [1–6]. Spinodal decomposition has been extensively characterised by Cahn [2, 7, 8] and others [3, 4, 9–13].

Because phase separation by nucleation and growth or by spinodal decomposition are by different processes, the morphology of the separated phases in each region are distinctly different. For nucleation and growth, the second phase particles tend to be spherical particles or have low connectivity. They tend to be of random size and distribution and a sharp boundary always exists between the two phases. For spinodal decomposition, the compositions of both phases vary with time until equilibrium is reached. The second phase tends to form non-spherical particles with high connectivity. The second phase is characterised by a regular distribution in size and position with a characteristic spacing and the boundary between phases is initially diffuse, but sharpens with time.

This study examines ionomer glasses of generic composition SiO_2-Al_2O_3-P_2O_5-CaO-CaF_2 and also a glass composition from the sodium-boro-silicate system.

The base ionomer glasses studied here contain large quantities of fluorides, which aid amorphous phase separation and can also result in controlled fluoride ion release [14]. These ionomer glasses can also be subjected to a controlled heat treatment which promotes the bulk nucleation of fluorapatite and mullite, leading to fine-grained, translucent, biocompatible glass-ceramics [15].

Ionomer glasses are believed to undergo metastable phase separation and there is some evidence of a spinodal decomposition process [16]. Hill *et al*. [16] used scanning electron microscopy to study a SiO_2-Al_2O_3-CaO-CaF_2 based glass composition. Prior to reaching the glass transition temperature, T_g the glass appeared featureless. After heating just past the glass transition, the glass exhibited an interconnected structure, suggesting that amorphous phase separation may be occurring by a spinodal decomposition mechanism. At higher temperatures the interconnected structure breaks down and a distinct droplet phase dispersed in a matrix phase is observed. The droplets appear to coarsen with time as the temperature increases.

Clifford *et al*. [17] investigated a closely related glass composition which also contained calcium fluoride. Transmission electron microscopy using a carbon-platinum replica technique demonstrated evidence of amorphous phase separation giving rise to an interconnected structure. The microstructure of one of the glasses following a 60 min heat treatment at the first peak crystallisation temperature, T_p1 exhibited crystals and the remains of an interconnected structure with crystal sizes varying from 0.4 to 0.8 μm.

An acid leaching study [18] of an ionomer glass provided evidence suggesting the presence of an interconnected structure. The pattern of ion release implied that the glass consisted of two interconnected phases or a spinodal structure and not a dispersion of discrete droplets of one phase in another. An EDX study by Moisescu [19] of an ionomer glass showed it to consist of an alumina-silica rich phase, which is relatively resistant to acid attack and a calcium-phosphate rich phase, which can be preferentially dissolved by acetic acid. The droplets possess sizes in the range of 200–500 nm. These droplets were found to increase in size and decrease in number on heating, owing to the phenomenon of Ostwald ripening [20]. The crystals formed possess sizes similar to that of the droplet phase and are formed when the droplet phase crystallises. Meanwhile Barry *et al*. [21] observed phase separation of SiO_2-Al_2O_3-CaO-CaF_2 ionomer glasses into two phases; one of which was more susceptible to acid attack. Barry *et al*. [21] observed droplet interconnectivity for a number of the glasses they studied.

The sodium-boro-silicate system [22], is widely known to undergo APS by a spinodal decomposition mechanism to generally give two interconnected glass phases, a sodium borate rich phase and a silica rich phase. The sodium-boro-silicate glass system forms the basis of the Vycor^{TM} process, which was the brainchild of two scientists, Hood and Nordberg of Corning Glass Works [23]. They found that objects made from certain alkali borosilicate glasses, after conversion into porous objects by acid leaching, could be subsequently sintered into reconstructed, pore-free, high silica glass [24]. A sodium-boro-silicate glass developed by Hammel *et al*. [25], which is well known to undergo APS, and has end applications as a microporous glass based on this phenomenon, is also investigated here.

The extent of the phase separation process and the pore size distribution and morphology of the leached borosilicate glass network is dependent on the heat treatment [22]. To develop a fully interconnected structure, heat-treatments of a few hours to several days at temperatures between 500°C and 600°C are required, and there is evidence that prolonged heat-treatment above 600°C will result in the coarsening of a finely interconnected system to that of droplets by diffusion-controlled agglomeration of the soluble phase. Scanning electron microscopy and transmission electron microscopy have been extensively used [29] to investigate the phenomenon of the interconnected structure in borosilicate glasses. Coarsening is attributed to further coalescence of the silica-rich phase into an interconnecting network caused by heating. These submicroscopic phases grow and increase in size with temperature and time [30].

2. Experimental procedure

Ionomer glasses containing SiO_2, Al_2O_3, P_2O_5, CaO and CaF_2 were systhesised. Table I shows the compositions of the ionomer glasses along with their respective firing temperatures and calcium phosphate (Ca/P) ratios. Approximately 800 g of each glass was synthesised in a single batch.

A fourth glass was also synthesised. This was a Sodium-Boro-Silicate glass containing 51.5 wt% SiO_2, 40 wt% B_2O_3 and 8.5 wt% Na_2O which was produced in accordance with a composition chosen from a patent by Hammel *et al*. [25]. About 800 g of glass was melted. This glass is known to phase separate into a silica-rich and a borate-rich phase upon suitable heat-treatment.

Glasses 1 and 2 are of the same series but differ in that glass 2 has less phosphate than glass 1. Glass 3 is of a different series and has a Ca/P ratio of 5:3 which is the ratio of calcium to phosphate in the apatite crystalline phase ($Ca_5(PO_4)_3F$). Both series contain a basic oxide in the form of CaO, which helps eliminate silicon tetrafluoride loss from the melt during firing [31].

The glasses were prepared using lidded high density mullite crucibles (Zedmark Refractories, Earlsheaton, Dewsbury, UK) and fired at 1420°C for 120 min. The

TABLE I Ionomer glass compositions studied in molar proportions

Glass	SiO_2	Al_2O_3	P_2O_5	CaO	CaF_2	Ca/P ratio	Melt temperature (°C)
1	4.5	3	1.6	3	2	1.40	1420
2	4.5	3	1.4	3	2	1.61	1420
3	4.5	3	1.5	3.5	1.5	1.67	1430

resulting glass melts were then shock quenched directly into water to produce frit. A quantity of this glass frit was then ground and sieved to particle size fractions of >45 μm to <15 μm for DTA/TGA analysis. Combined DTA/TGA was used to measures values for the glass transition (T_g) and the peak crystallisation temperatures (T_p) in the glasses, as well as any weight changes that might occur during melting and crystallisation of phases. A Stanton Redcroft DTA/TGA 1600 (Rheometric Scientific, Epsom, UK) was used with a flowing dry nitrogen atmosphere and a heating rate of 10°K. min^{-1}. The sample and reference material were held in matched pairs of platinum-rhodium alloy crucibles.

High temperature DMTA was used as means of investigating APS. This technique measures the viscoelastic damping (tan δ) of glassy phases, with each glassy phase manifesting itself as a reduction in the storage modulus and a peak in damping factor, tan δ, as a function of temperature. In this way glass transitions can be accurately determined. Crystallisation processes, which give rise to changes in the modulus of the glass may also be monitored using this technique. The DMTA apparatus used was a Polymer Laboratories High Temperature DMTA MK III (Thermal Sciences Division, Loughborough, UK), with a maximum furnace head temperature of 800°C. Glass frit was recast in alumina crucibles (VZS Technical Ceramics, Glenroites, Fife, Scotland) and poured onto a pre-heated sheet of steel. The resulting glass pats were then annealed for 240 min at 50°C below T_g. Glass bars measuring approximately 6 × 2 × 30 mm were cut using a diamond edged flitting wheel and ground down and polished to a 1 μm finish to remove surface cracks. In this way almost perfectly flat samples were produced, which is vital for successful performance of the DMTA instrument. For a detailed description of the DMTA technique the reader is referred to a very recent study by this author [32] and also an earlier study by Hill *et al.* [33].

Ionomer glasses and sodium-boro-silicate samples were heat-treated to various temperatures using an Austromat 3001 Dental Porcelain Furnace (Austromat®-Keramikofen, D-83395 Freilassing, Germany). The microstructure of the phase separated glasses was investigated using an Hitachi S-4100 Field Emission Scanning Electron Microscope (Hitachi, Japan). The samples were fractured and etched for 10 seconds in 10% HNO_3. An SEM coating unit E5000 (Polaron Equipment Ltd. England) was used to gold coat the samples prior to examination.

3. Results and discussion

Combined DTA/TGA analysis was carried out on the sodium-boro-silicate glass composition. Fig. 1 is a DTA/TGA trace of the base glass, prior to any heat treatment.

From Fig. 1 the most noticeable features are two distinct endotherms at 183°C and 203°C respectively. These are thought to be due to the volatilisation of absorbed water and other contaminants. Porous vycor

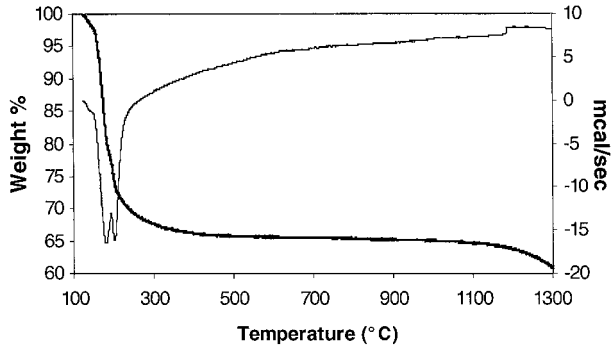

Figure 1 DTA/TGA trace of sodium-boro-silicate base glass.

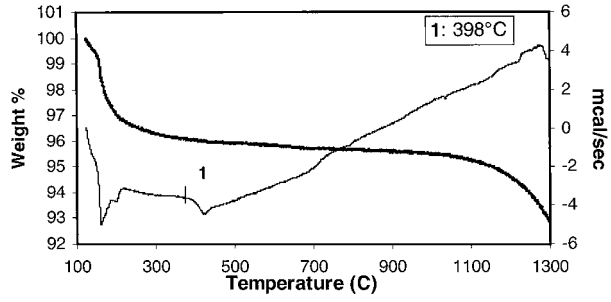

Figure 2 DTA/TGA trace of sodium-boro-silicate glass after heat-treatment at 580°C for 240 min.

glass is commonly known as "thirsty glass" because of its affinity for moisture. There is a 35% weight loss associated with this moisture loss indicating that the glass had taken up a considerable amount of atmospheric water in the month prior to analysis. It can be seen from Fig. 1 that there no clear evidence of a glass transition for the base glass. A sample of the sodium-boro-silicate glass was then heat-treated for 240 min at 580°C, in accordance with the guidelines in the patent [25]. A DTA/TGA trace for the heat-treated sample is shown in Fig. 2.

Again there are two distinct endotherms at 183°C and 203°C. These are less prominent than for the base glass, as the temperature hold for 240 min at 580°C has probably volatilised a large amount of this moisture already. There is only a 3% weight loss associated with these transitions. The most obvious feature of this trace however is the change in slope at approximately 398°C, corresponding to a glass transition. It would appear that the temperature hold has caused the glass to phase separate into two amorphous phases, a sodium-borate rich phase and a silica phase. The glass transition seen in Fig. 2, because of its low transition temperature, is probably due to the presence of the sodium-borate rich glass phase, as the glass transition of the silica glass phase would be expected at much higher temperatures. Ray [34], in a review which regards simple inorganic oxide glasses as ionic polymers, suggests a transformation temperature of 1200°C for SiO_2. The absence of a clear glass transition temperature in the as quenched sodium borosilicate glass is surprising. The failure to detect a glass transition temperature in the as quenched glass may be due to there being a critical phase size required in order to detect a separate glass transition temperature for the sodium borate rich glass phase. The complete absence

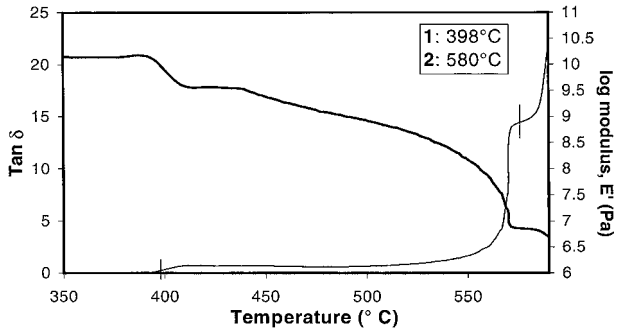

Figure 3 Storage modulus, E′ (▬), and tan δ (—) for the sodium-boro-silicate base glass.

of a glass transition in the base glass may be due to the glass phase separating during the DSC run.

High temperature DMTA analysis was carried out on the sodium-boro-silicate base glass, the result of which is shown in Fig. 3.

A rise in tan δ at approximately 395°C is seen to occur which is accompanied by a drop in the storage modulus, E′. The rise in tan δ at approximately 395°C is due to the presence of a sodium-borate rich glass phase and is in very good agreement with the glass transition temperature of 395°C observed from the DTA/TGA for the heat-treated glass. A shoulder occurs in the second tan δ peak at approximately 580°C. This is heat-treatment temperature used in the patent by Hammel *et al*. [25] and it is believed that the phase separation process is at an advanced stage at this point. The point at approximately 600°C is believed to be the point where the glass begins to flow.

Mazurin [35], using a torsion pendulum apparatus built by Duke and Douglas [36] found a pronounced relaxation peak at 470°C for a heat-treated borosilicate glass of composition (mol%: $3.9Na_2O31.2B_2O_364.9SiO_2$). Interestingly, no peak was found for the sample drawn directly from the melt. According to Mazurin, this glass composition will form, after a suitable heat-treatment, isolated inclusions of a highly conductive (low viscosity) phase and, therefore, the high viscosity phase in such glasses is continuous. This high-viscosity phase must be continuous in order to see a relaxation peak. Mazurin concludes that in a rapidly chilled glass of given composition there is no framework of the high viscosity phase, and this framework is formed only during heat treatment.

On the basis of Mazurin's findings it would appear that the peak found for the sodium-boro-silicate (Hammel) glass at 398°C is analogous to the one found at 470°C for Mazurin's glass composition. Likewise, Mazurin also found that the internal friction or tan δ rose steadily from 500°C onwards, though the upper temperature limit of the curve was fixed by the deformation of the glass fibre under the weight of the inertia beam to which it was attached.

Scanning electron microscopy of the sodium-boro-silicate glass was conducted and a classical interconnected structure consisting of two mutually penetrating interconnected phases was observed. Fig. 4 is an

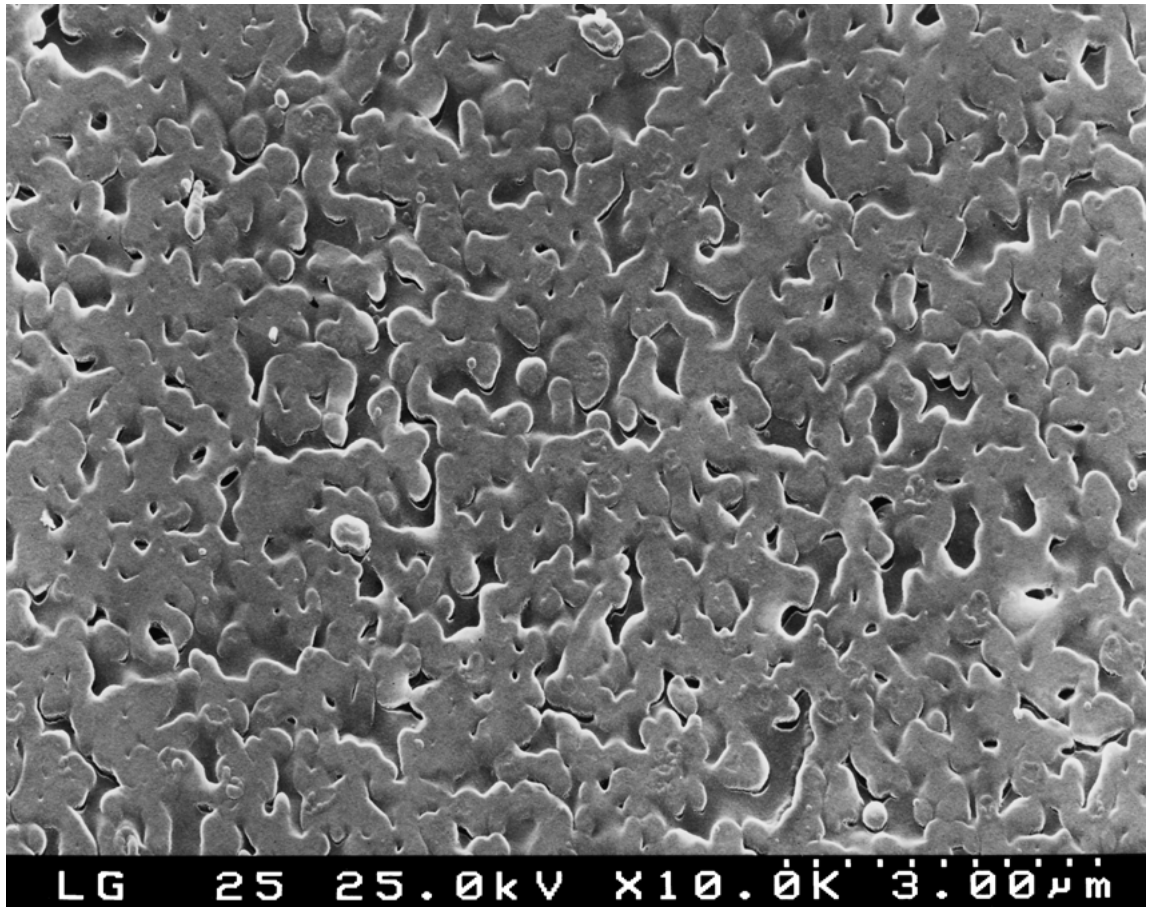

Figure 4 SEM of sodium-boro-silicate glass, heat-treated 240 min at 580°C X10 K.

SEM of the sodium-boro-silicate glass that had been heat-treated for 240 min at 580°C.

This structure closely resembles interconnected structures observed by authors such as Strnad [37], Haller [38], and Cahn [2, 39]. The pore structure ranges from approximately 20 nm in narrow sections up to 400 nm in the wider sections.

According to McMillan [40], for spinodal decomposition the compositions of both phases vary with time until equilibrium is reached. The second phase tends to form non-spherical particles with high connectivity. The second phase is characterised by a regular distribution in size and position with a characteristic spacing and the boundary between phases is initially diffuse, but sharpens with time. It is a spinodal decomposition mechanism that is taking place for the sodium-boro-silicate glass composition.

Combined DTA/TGA up to 1300°C was carried out for the ionomer base glass compositions. All of the base ionomer glasses show two distinct crystallistation peaks. Previous XRD studies by Hill and Wood [41] of glasses with Ca/P ratio between 1.25 and 2 showed them to crystallise to fluorapatite ($Ca_5(PO_4)_3F$) and mullite ($3Al_2O_32SiO_2$). Anorthite ($2SiO_2$ Al_2O_3CaO) has previously been shown to occur in glass compositions with calcium to phosphate ratios of 1.67 that contain no fluorine. Mullite, which is a high temperature refractory phase, is formed at unusually low temperatures in these glasses and this may suggest that there are other components present in the aluminium-silicon rich phase.

All of the base ionomer glasses show a distinct endotherm at approximately 1250°C. Fig. 5 shows the DTA/TGA trace recorded for glass 2, which is typical of the other ionomer glasses.

A change in slope occurs at approximately 640°C corresponding to the glass transition. An endotherm is detected at approximately 1250°C, and is believed to be due to the transformation of mullite into anorthite. The weight loss following crystallisation is attributed to volatile silicon tetrafluoride and starts to occur at a temperature corresponding to T_p1 onset. The loss of silicon tetrafluoride occurs from the surface following crystallisation and is probably associated with the local bonding of fluorine. It is thought that in the present glasses fluorine bonds to the aluminium in the glass network, replacing a bridging oxygen by two non-bridging fluorine atoms. Following

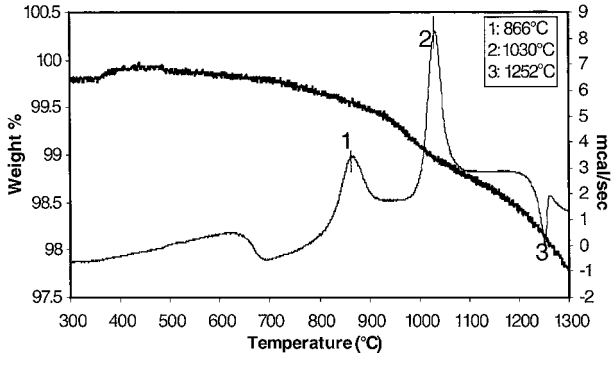

Figure 5 DTA/TGA trace of glass 2.

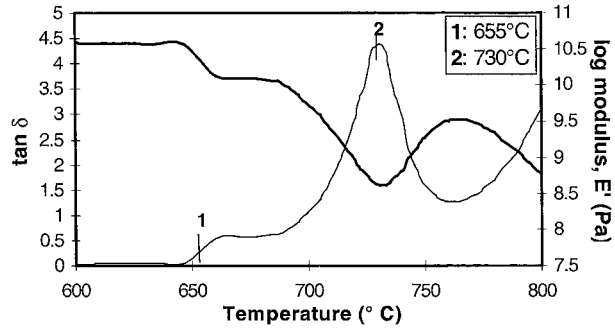

Figure 6 Storage modulus, E′ (▬), and tan δ (—) for glass 2.

crystallisation of apatite however, and the removal of non-bridging oxygens connected to silicon atoms, it is likely that fluorine will bond to silicon atoms in preference to aluminium atoms, resulting in the formation of Si–F bonds and the possibility of silicon tetrafluoride formation [14]. Previous DTA/TGA studies of fluoro-alumino-silicate glass compositions have shown weight losses accompanying crystallisation [42, 43], and for this weight loss to disappear in fluorine free compositions.

DMTA of glass 2 was conducted. Fig. 6 shows the damping factor, tan δ and storage modulus, E′ as a function of temperature. An almost identical trace was recorded for glass 1.

There is a rise in tan δ at approximately 655°C. This is typical of a glass transition and ties in with the value for T_g observed in the DTA/TGA data of Fig. 6. It is believed to be a glass transition for a calcium-phosphate rich phase. A second loss peak is observed at approximately 730°C. This is believed to be due to a second glass phase, most likely an aluminium-silicon rich glass phase. Moisescu [44] conducted EDX of ion-thinned samples of apatite containing ionomer glasses of similar composition to those studied here and confirmed a calcium-phosphate rich droplet phase and a glass matrix enriched in SiO_2 and Al_2O_3. From approximately 760°C onwards a rise in E′ is seen to occur corresponding to crystallisation of the glass. This temperature range corresponds to T_p1 onset for this glass as seen in the DTA/TGA trace of Fig. 5. A similar rise in E′, for glasses in the Li_2O-ZnO-SiO_2 system [33] was found to be due to crystallisation of the glass, and again agreed broadly with related DSC data.

Scanning electron microscopy of glass 2 was conducted to find evidence for two amorphous phases. On this occasion the glass had been subjected to a 60 min hold at a pre-determined optimum nucleation temperatures which were pre-determined using the Marotta method [45, 46]. See Figs 7 and 8.

The micrographs reflect closely those found for base glass 1. See Figs 9 and 10.

A number of sparse droplets, ranging in size between approximately 20 and 100 nm can be seen. The background to the droplets has a somewhat speckled appearance and it is unclear why this is so and if indeed there may be some type of phase separated structure here also. Hill *et al.* [16] investigated a SiO_2-Al_2O_3-CaO-CaF_2 composition and found an interconnected

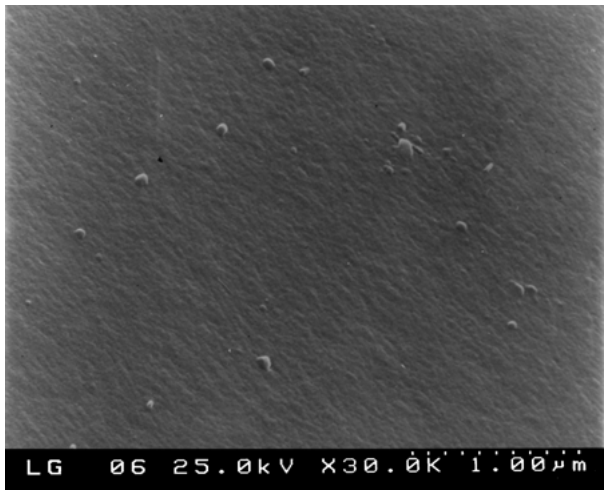

Figure 7 SEM micrograph of glass 2, heat-treated for 60 min at the optimum nucleation, temperature X30 K.

structure, while at higher temperatures a distinct droplet in matrix structure emerged. James [47], in a review of APS in inorganic glasses postulates that for some glass systems the effective spinodal boundary may be depressed to lower temperatures and samples would always have to traverse a nucleation region before reaching the spinodal. It may be that the droplets observed are formed on traversing the metastable gap between the spinodal and binodal, whilst the speckled background is due to fine scale APS occurring within the spinodal.

The volume fraction of the droplet phase is very small. It would appear that this is being reflected in the DMTA trace of glass 2 where the second rise in tan δ is approximately ten times greater in magnitude than that of the first rise in tan δ. This would only be true if the first lower temperature peak corresponded to a calcium-phosphate rich phase and the second higher temperature peak to an aluminium-silicon rich phase, which is believed to be the case. From XRD measurements these glasses were shown to crystallise firstly to fluorapatite ($Ca_5(PO_4)_3F$) at approximately 850°C followed by mullite ($3Al_2O_32SiO_2$) at much higher temperatures in excess of 1000°C. This reinforces the view of a calcium phosphate phase crystallising to fluorapatite and an aluminium-silicon rich phase crystallising to mullite.

DMTA of glass 3 was carried out and is interesting when compared to glasses 1 and 2. See Fig. 11.

Firstly, the amplitudes of the two maxima in tan δ are a great deal lower than for glasses 1 and 2. The rise in tan δ at approximately 654°C is of a similar magnitude to the rise in tan δ for the second peak at 707°C suggesting that the volume fractions of the glass phases could be present in approximately equal proportions. This is in contrast to glasses 1 and 2 where the magnitude of the rise of the second tan δ peak is of the order of ten times greater than that of the first tan δ peak.

Scanning electron microscopy of glass 3 confirmed that this glass has a very large volume fraction of droplets as shown in Fig. 12.

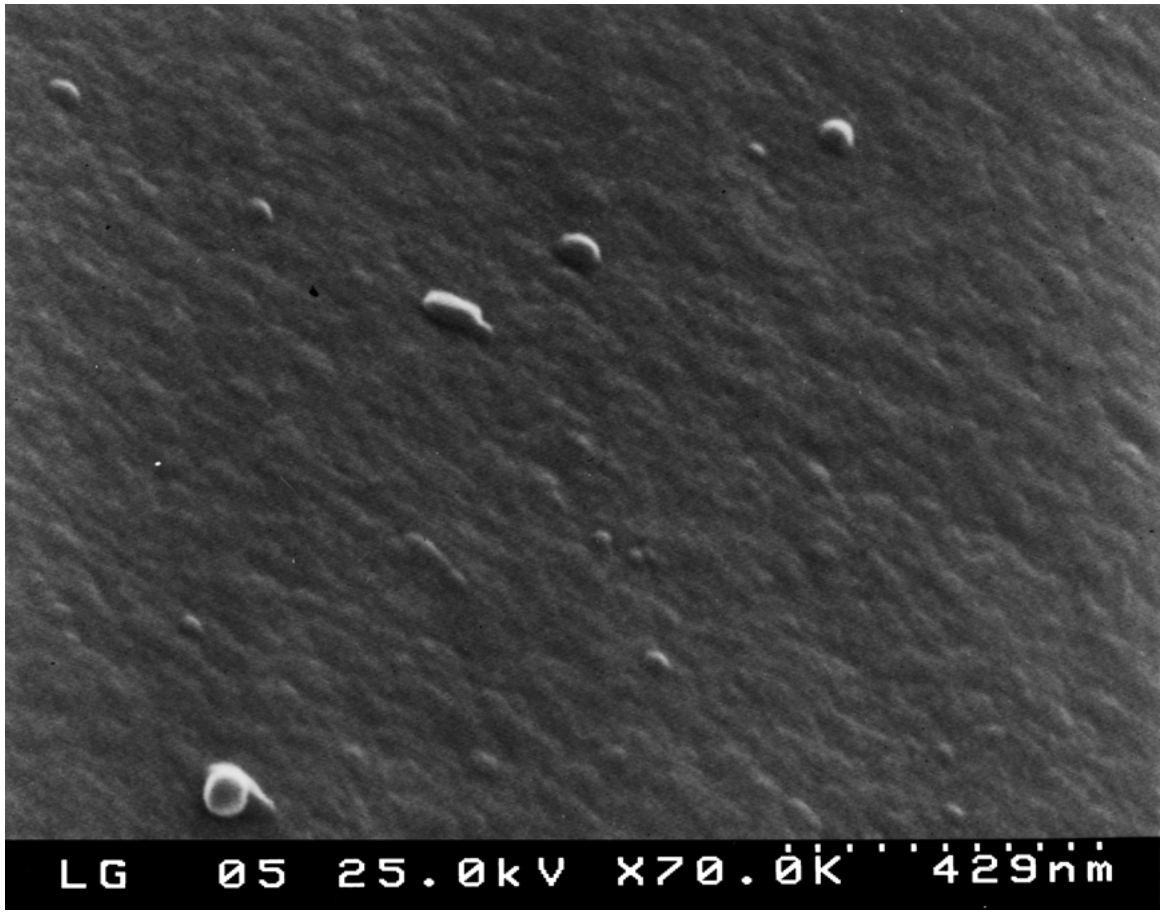

Figure 8 SEM micrograph of glass 2, heat-treated for 60 min at the optimum nucleation temperature, X70 K.

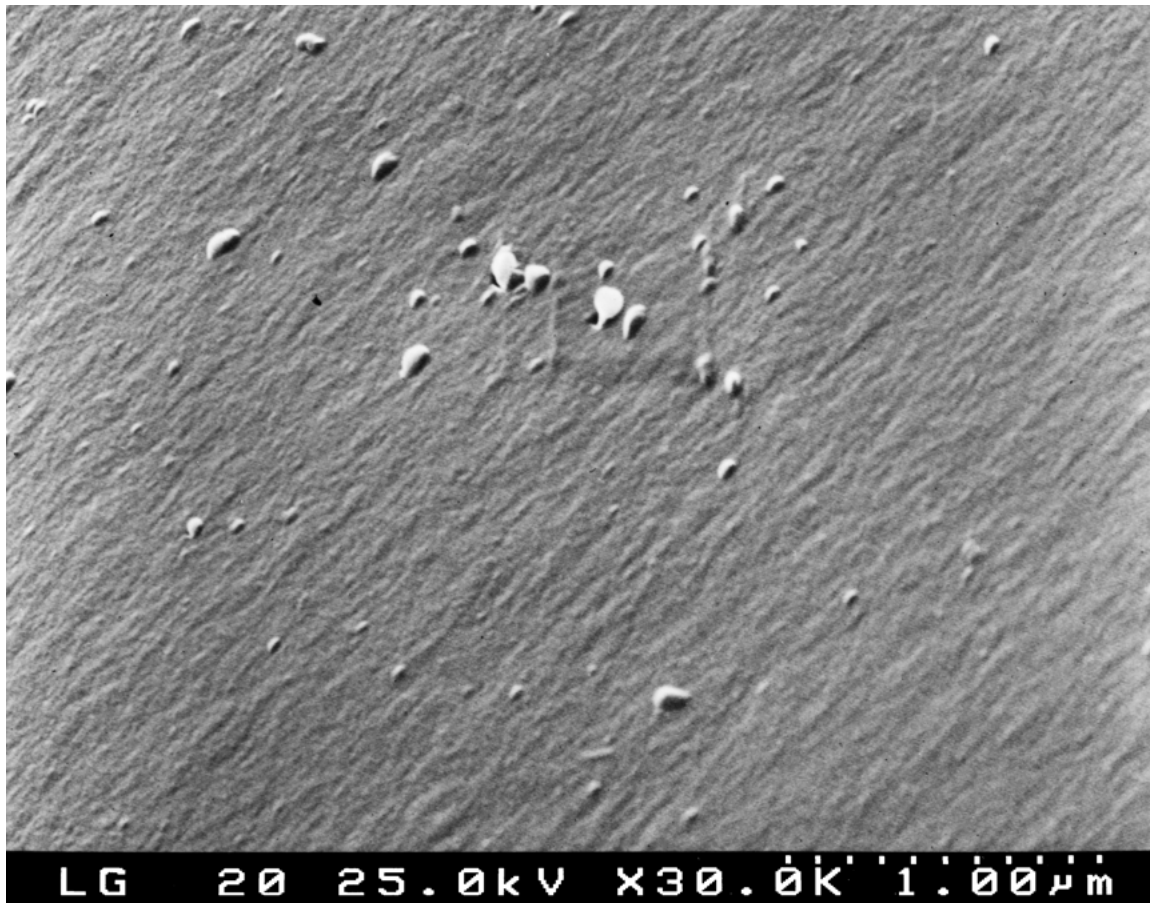

Figure 9 SEM micrograph of glass 1, X30 K.

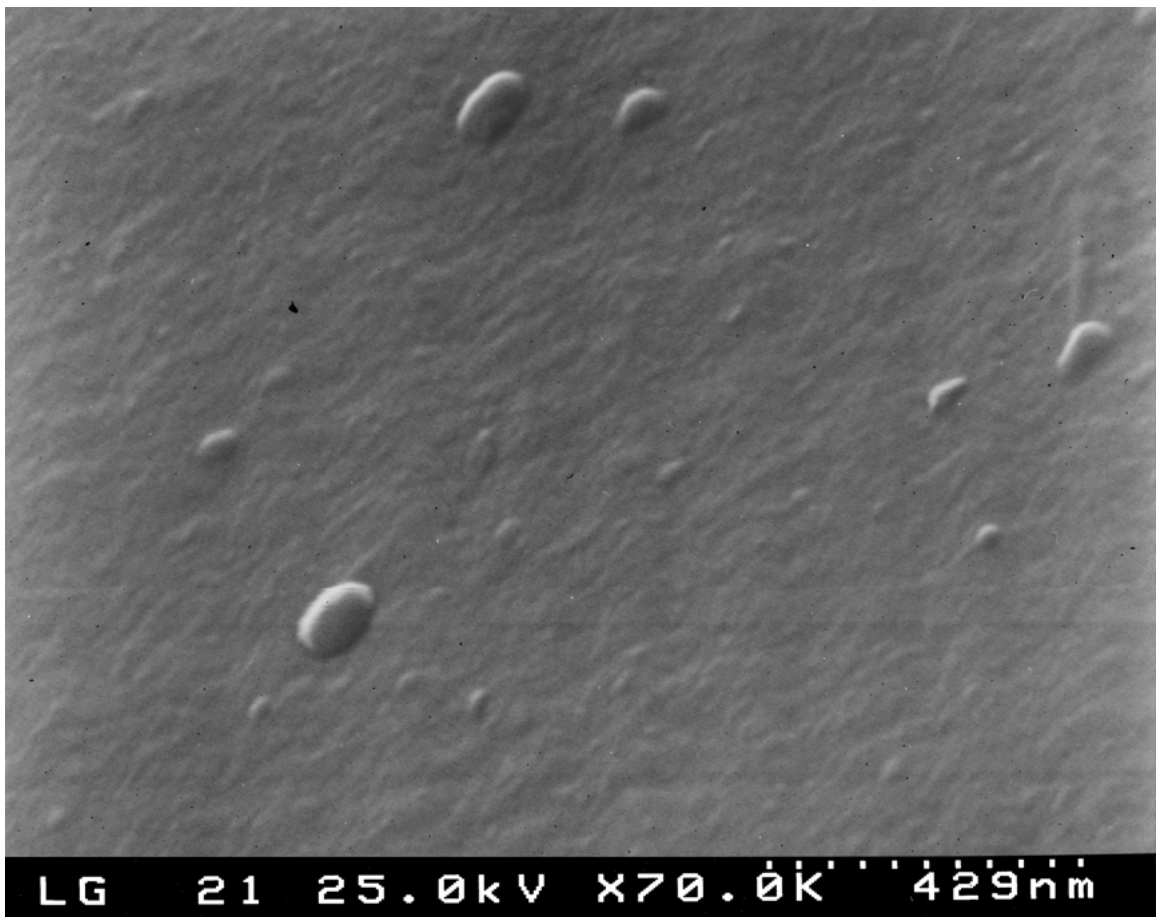

Figure 10 SEM micrograph of glass 1, X70 K.

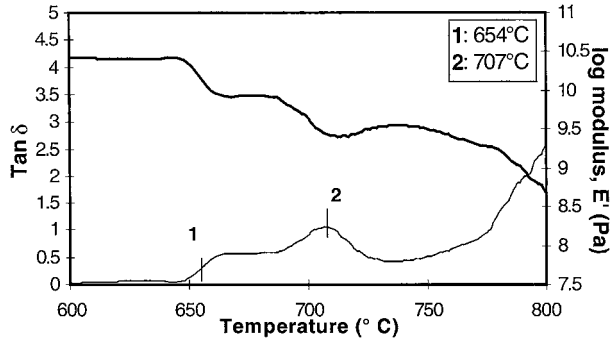

Figure 11 Storage modulus, E′ (▬) and tan δ (—) for glass 3.

Glass 3 possesses the structural unit of the crystalline phase, (Ca/P = 1.67) and although disordered, the degree of movement and structural rearrangement required for crystallisation should be lower than for the other glasses. A lower degree of structural rearrangement will mean, of course less internal deformation and lower amplitudes in tan δ. The first peak in tan δ is again believed to be due to a calcium-phosphate rich phase. The second peak is believed to correspond to an aluminium-silicon rich phase but the maximum in tan δ corresponding to the glass transition at 707°C is quite low and would suggest that there are other components present in the aluminium-silicon rich phase. Earlier, it was also noted that mullite is formed at unusually low temperatures in these glasses, as was seen from the position of T_p2 from DTA/TGA analysis.

4. Conclusions

Fluorine and phosphate play an important role in determining APS and subsequent bulk nucleation in ionomer glasses. DTA/TGA showed that fluorine containing glasses suffered weight losses of only 1–3% due to silicon tetrafluoride formation, while glasses with no fluorine are known to exhibit negligible weight loss.

High temperature dynamic mechanical thermal analysis was used to study structural changes in both ionomer glasses and a sodium-boro-silicate glass. High temperature DMTA showed the presence of two glass transition temperatures for the three ionomer glasses, demonstrating that APS had occurred. DMTA traces of two of the ionomer glasses of the same series and of similar composition were in good agreement. Both exhibited two maxima in tan δ, the second of which was approximately ten times in magnitude to that of the first. This indicated the presence of a small volume fraction of one glass phase and a much larger volume fraction of another. It is believed that the low volume fraction phase is calcium-phosphate rich while the high volume fraction phase is aluminium-silicon rich.

Scanning electron microscopy of the ionomer glasses showed the presence of sparse droplets (20–100 nm). The second phase droplets were spherical and had a random distribution, suggesting a separation mechanism involving nucleation and growth. The background between the droplets had a speckled appearance but it was unclear from SEM alone whether a fine scale interconnected structure could also be present, as was

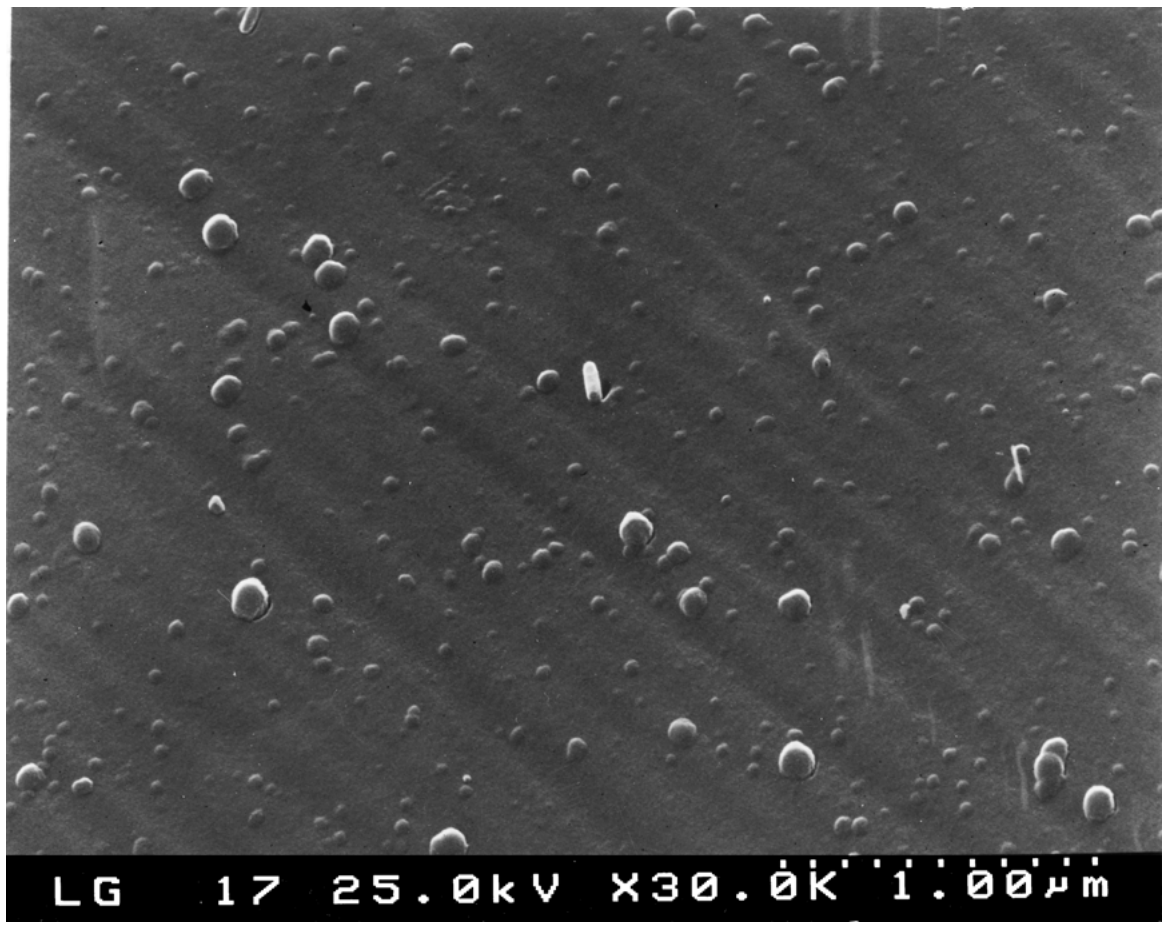

Figure 12 SEM micrograph of glass 3, heat-treated to Tp1-50, X30 K.

evidenced by previous authors [16–18, 21]. DMTA of a third ionomer glass with the fluorapatite Ca/P ratio ratio of 1.67 exhibited two rises in tan δ of similar amplitude, suggesting that this glass had similar volume fractions of the glass phases present. This was confirmed by scanning electron microscopy.

A sodium-boro-silicate glass which is well known in the patent literature to undergo APS was also shown to exhibit two rises in tan δ, the first of which occurred at ~395°C and was due to a sodium-borate rich phase. The results, when compared with those for the ionomer glasses studied, support the view that nucleation is via prior amorphous phase separation. The sodium-boro-silicate glass exhibited a classical interconnected structure with a continuous phase present when examined using SEM. The base sodium-boro-silicate glass showed no glass transition by DTA/TGA. However, after a heat-treatment of 240 min at 580°C, a clear T_g emerges at approximately 395°C and this was in good agreement with the temperature of the tan δ peak from DMTA analysis. This is believed to be due to the coarsening up of an already phase-separated glass to a size greater than the size scale of the parts of the glass network associated with the glass transition.

Acknowledgements

The authors would like to gratefully acknowledge the support of Brite EuRam Contract BRPR-CT96-0230. The authors would also like to thank M. Olivieira, Departamento de Engenharia Ceramica E Do Vidro, Universidade de Aveiro, 3810 Aveiro, Portugal. for his technical assistance with the Field Emission Scanning Electron Microscope.

References

1. P. F. JAMES "Glasses and Glass-Ceramics" (Chapman and Hall, London, 1989).
2. J. W. CAHN and R. J. CHARLES, *Phys. Chem. Glasses* **6** (1965) 181.
3. D. R. UHLMANN and A. G. KOLBECK, *ibid.* **17** (1976) 146.
4. W. VOGEL, *J. Non. Crys. Solids* **25** (1977) 170.
5. N. KREIDL, *ibid.* **129** (1991) 1.
6. M. C. WEINBERG, V. A. SHNEIDMAN and Z. A. OSBORNE, *Phys. Chem. Glasses* **37** (1996) 49.
7. J. W. CAHN, *Trans. Metal. Soc. AIME* **242** (1968) 165.
8. R. B. HEADY and J. W. CAHN, *J. Chem. Phys.* **58** (1973) 896.
9. R. W. HASKELL, *J. Amer. Ceram. Soc.* **56** (1973) 355.
10. C. M. JANTZEN, D. SCHWAHN, J. SCHELTEN and H. HERMAN, *Phys. Chem. Glasses* **22** (1981) 122.
11. G. F. NEILSON, *ibid.* **10** (1969) 54.
12. J. ZARZYCKI, F. NAUDIN, *J. Non. Crys. Solids* **1** (1969) 215.
13. T. P. SEWARD, D. R. UHLMANN, D. TURNBULL, *J. Amer. Ceram. Soc.* **51** (1968) 634.
14. A. RAFFERTY, A. CLIFFORD, R. HILL, D. WOOD, B. SAMUNEVA and M. DIMITROVA-LUKACS, *ibid.* **83** (2000) 2833.
15. R. HILL, A. RAFFERTY, P. MOONEY and D. WOOD, *Glastech. Ber. Glass Sci. Technol* **73** (2000) Suppl C1, 146.
16. R. G. HILL, C. GOAT and D. WOOD, *J. Amer. Ceram. Soc.* **75** (1992) 778.
17. A. CLIFFORD, R. HILL, A. RAFFERTY, P. MOONEY, D. WOOD, B. SAMUNEVA and S. MATUSUYA, *J. Mater. Sci. Mats: In Med.* **12** (2001) 461.
18. E. A. WASSON and J. W. NICHOLSON, *Brit. Poly. J.* **23** (1990) 179.
19. C. MOISESCU, C. JANA and C. RÜSSEL, *J. Non. Cryst. Solids* **248** (1999) 169.
20. C. JANA and W. HÖLAND, *Silicates Industriels* **56** (1991) 215.
21. T. I. BARRY, D. J. CLINTON, L. A. LAY and R. P. MILLER, ASPA Dental Cement NPL Report; Part 1. (1972) 1.
22. N. FORD and R. TODHUNTER, "Glasses and Glass Ceramics" (Chapman and Hall, 1989).
23. H. P. HOOD and M. E. NORDBERG, US Patent no. 2,196,744, (1934).
24. D. R. UHLMANN and N. J. KREIDL, "Glass-Science and Technology," Vol. 1.
25. J. HAMMEL and T. ALLERSMO, US Patent no. 3,972,721 (Aug. 3, 1976).
26. J. HAMMEL and T. ALLERSMO, US Patent no. 3,972,720 (Aug. 3, 1976).
27. H. P. HOOD and M. E. NORDBERG, US Patent no. 2,196,744 (1934).
28. N. FORD and R. TODHUNTER, "Glasses and Glass Ceramics" (Chapman and Hall, 1989).
29. W. HALLER and P. B. MACEDO, *Phys. Chem. Glasses* **5** (1968) 153.
30. T. H. ELMER, "Engineered Materials Handbook," Vol. 4 (ASM International, USA, 1991) p. 427.
31. D. WOOD and R. HILL, *Clin. Mater.* **7** (1991) 301.
32. A. RAFFERTY, R. HILL and D. WOOD, *J. Mater. Sci.* **35** (2000) 1.
33. R. HILL and P. GILBERT, *J. Amer. Ceram. Soc.* **76**(2) 25 (1993) 417.
34. N. H. RAY, *Brit. Poly. J.* **7** (1975) 307.
35. O. V. MAZURIN, *Phys. Chem. Glasses* **9** (1968) 165.
36. R. W. DOUGLAS, P. J. DUKE and O. V. MAZURIN, *ibid.* **9** (1968) 169.
37. Z. STRNAD, "Glass-Ceramic Materials" (Elsevier Science Publishing Company Inc., Amsterdam, 1986).
38. W. HALLER and P. B. MACEDO, *Phys. Chem. Glasses* **5** (1968) 153.
39. J. W. CAHN and J. E. HILLIARD, *J. Chem. Phys.* **28** (1958) 258.
40. P. W. MC MILLAN, "Glass Ceramics" (Academic Press, London, 1979).
41. D. J. WOOD and R. G. HILL, *Clin. Mats.* **7** (1991) 301.
42. D. WOOD, PhD thesis, University of Greenwich, 1992.
43. P. MOONEY, MSc. PhD Transfer Report, University of Limerick, 1997.
44. C. MOISESCU, C. JANA, S. HABELITZ, G. CARL and C. RÜSSEL, *J. Non. Cryst. Solids* **248** (1999) 176.
45. A. MARROTTA, A. BURI, F. BRANDA and S. SAILLO, "Nucleation and Crystallisation in Glasses" (American Ceramic Society Inc. Ohio, 1982) p. 145.
46. A. MARROTTA, A. BURI and F. BRANDA, *J. Mater. Sci.* **16** (1981) 341.
47. P. F. JAMES, *J. Mats. Sci.* **10** (1975) 1802.

Received 13 August 2002
and accepted 4 February 2003